Pure Appl. Opt. **5** (1996) 141–156. Printed in the UK

Some topics in extending the C method to multilayer gratings of different profiles

Lifeng Li†, G Granet‡, J P Plumey§ and J Chandezon§

† Optical Sciences Center, University of Arizona, Tucson, AZ 85721, USA
‡ INT, 9 rue Charles Fourier, 91011 Evry Cedex, France
§ LASMEA URA 1793, Université Blaise Pascal, 63177 Aubière Cedex, France

Received 29 June 1995, in final form 11 September 1995

Abstract. In a recent Letter to the Editor (1995 *Pure Appl. Opt.* **4** 1–5), the differential formalism of Chandezon *et al* (the C method) was extended to treat layered gratings in which the profiles of the medium interfaces within the same grating are different from each other. Numerical experiments have shown that a computer program based on the recipe given in the Letter gives excellent numerical results for diffraction efficiencies. However, a crucial assumption was implicitly used without justification. In this paper, we examine this assumption and comment on its validity. In addition, we suggest two alternative ways to extend the C method, and show that one of them is as effective as the recipe given in the Letter.

1. Introduction

The original differential formalism of Chandezon *et al* [1, 2] (henceforth, the C method) has been proven to be a powerful method for modelling multilayer-coated diffraction gratings in the entire optical region. However, it was only applicable to the case in which all contours of the medium interfaces of a grating have the same functional form and amplitude. This is a severe limitation because in reality the medium interfaces of coated gratings never perfectly follow each other. Moreover, in some applications the interface profiles are intentionally shifted relative to each other in the direction of the grating vector [3].

Recently, Granet *et al* [4] extended the C method to allow the periodic medium interfaces to have different functional forms and amplitudes. Numerical experiments have shown that a computer program based on the procedure suggested in [4] gives excellent numerical results for diffraction efficiencies. However, in the theoretical presentation of [4], a crucial assumption was implicitly used without justification. Basically, this assumption asserts that, throughout a medium between two interfaces the sum of all upward (downward) propagating waves and upward (downward) decaying waves expressed in terms of the eigensolutions of Maxwell's equations in one coordinate system is equal to a similar sum expressed in the other coordinate system. In this paper, we carefully examine the validity or invalidity of this assumption. In addition, we suggest two alternative ways to extend the C method, and show that one of them is as effective as the extension suggested by Granet *et al*.

2. Background information

Here, we only give the mathematical formulae of the C method to the extent necessary for the reader to follow the discussions in the subsequent sections. A reader who is not familiar

0963-9659/96/020141+16$19.50

with the original C method is referred to [1] and [2] for more background information. To achieve maximum clarity and ease of reading, we use a notation that is substantially different from that used in [4].

Without loss of generality, we only consider the non-conical mount and the TE polarization (electric field vector parallel to the grating grooves). The Gaussian system of units and the harmonic time convention $\exp(-i\omega t)$ are used. The magnetic permeability is assumed to be unity everywhere. The Cartesian coordinate system and the notation for the media and medium interfaces are illustrated in figure 1. For the sake of simplicity, only two representative adjacent interfaces are shown. The interfaces in general have different functional forms and amplitudes, but they share a common period d. The thickness e_p of layer p is measured between the mid lines of the two boundaries.

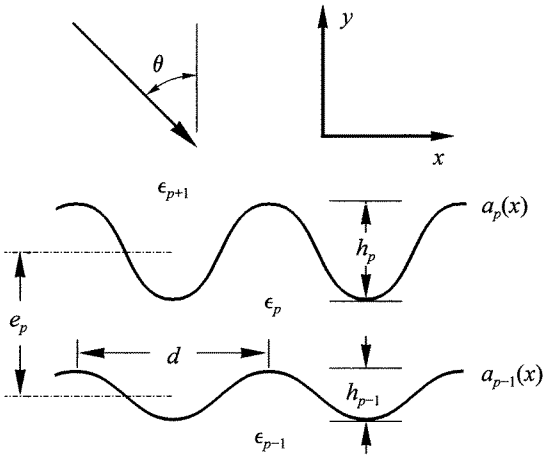

Figure 1. Notation for the description of a layered grating.

In contrast to the original C method, where one curvilinear coordinate system applies to all periodic interfaces, in the present case every interface $a_p(x)$ generates a curvilinear coordinate system:

$$x_p = x \qquad u_p = y - a_p(x) \qquad z_p = z\,. \tag{1}$$

Thus, the interface represented by $y = a_p(x)$ is given by $u_p = 0$. Whenever there is no danger of causing confusion, we will drop the subscript for variable x and z. However, the reader should bear in mind that the direction of unit vector $\hat{x}_p$ depends on p.

We denote all matrix quantities that depend on both the medium and the coordinate system by using a pair of superscripts enclosed in parentheses, the first superscript for the medium number, and the second for the coordinate system in which the eigensolutions are obtained, leaving the subscripts for labelling the matrix elements. For quantities that depend only on the coordinate system, a single superscript enclosed in parentheses is used. For scalar quantities, subscripts are used, except for the vector components of the fields printed in bold face. Following the tradition of the C method, we have

$$\boldsymbol{F}^{(p,q)}(x, u_q) = \boldsymbol{E}_z^{(p,q)}(x, u_q) \tag{2a}$$

$$\boldsymbol{G}^{(p,q)}(x, u_q) = \kappa \boldsymbol{H}_{x_q}^{(p,q)}(x, u_q) \tag{2b}$$

where κ is the vacuum wavenumber.

In the C method, Maxwell's equations are written in a covariant form and the electromagnetic fields are expanded in Fourier series. This procedure leads to a matrix algebraic eigenvalue problem (in a spatial region where the permittivity is a constant):

$$M^{(p,q)}\begin{pmatrix} F_m^{(p,q)} \\ G_m^{(p,q)} \end{pmatrix} = \lambda^{(p,q)}\begin{pmatrix} F_m^{(p,q)} \\ G_m^{(p,q)} \end{pmatrix} \tag{3}$$

where $\lambda^{(p,q)}$ is the eigenvalue, $F_q^{(p,q)}$ and $G_m^{(p,q)}$, together as the eigenvector, are the u_q independent Fourier coefficients of $F^{(p,q)}$ and $G^{(p,q)}$, and $M^{(p,q)}$ is a complex matrix whose definition can be found, for example, in [2]. Here, we have used a typical element, e.g. $F_m^{(p,q)}$, to represent the whole sub-column vector. This type of short-hand notation will be used frequently in this paper.

We partition the full eigenvalue spectrum $\sigma^{(p,q)}$ of $\lambda^{(p,q)}$ as follows:

$$\sigma^{(p,q)} = \sigma^{(p,q)+} \cup \sigma^{(p,q)-} \tag{4}$$

where

$$\sigma^{(p,q)+} = \{\lambda_m^{(p,q)}; \operatorname{Re}\lambda_m^{(p,q)} + \operatorname{Im}\lambda_m^{(p,q)} > 0, \forall m\} \tag{5a}$$

$$\sigma^{(p,q)-} = \{\lambda_m^{(p,q)}; \operatorname{Re}\lambda_m^{(p,q)} + \operatorname{Im}\lambda_m^{(p,q)} < 0, \forall m\}\,. \tag{5b}$$

It can be shown that for any truncation of $M^{(p,q)}$ to a finite size, $\sigma^{(p,q)+}$ and $\sigma^{(p,q)-}$ have the same number of elements. From now on, we denote quantities corresponding to $\sigma^{(p,q)\pm}$ by subscripts or superscripts $\pm$. Also, we call an eigensolution of equation (3) associated with $\lambda^{(p,q)+}$ an up-wave and that associated with $\lambda^{(p,q)-}$ a down-wave. From equation (5), an up- (down-) wave is either propagating or decaying in the upward (downward) direction. The sum of all up- (down-) waves can be written as:

$$\boldsymbol{F}_{\pm}^{(p,q)}(x, u_q) = \sum_{m,n} \mathrm{e}^{\mathrm{i}\alpha_m x} F_{mn}^{(p,q)\pm} \mathrm{e}^{\mathrm{i}\lambda_n^{(p,q)\pm} u_q} v_n^{(p,q)\pm} \tag{6a}$$

$$\boldsymbol{G}_{\pm}^{(p,q)}(x, u_q) = \sum_{m,n} \mathrm{e}^{\mathrm{i}\alpha_m x} G_{mn}^{(p,q)\pm} \mathrm{e}^{\mathrm{i}\lambda_n^{(p,q)\pm} u_q} v_n^{(p,q)\pm} \tag{6b}$$

where $(F_{mn}^{(p,q)\pm}, G_{mn}^{(p,q)\pm})$ and $v_n^{(p,q)\pm}$ are the eigenvector and its amplitude, respectively, corresponding to eigenvalue $\lambda_n^{(p,q)\pm}$, and α_m is defined conventionally

$$\alpha_m = \alpha_0 + mK \qquad \alpha_0 = k_{\mathrm{i}} \sin\theta \qquad K = 2\pi/d \tag{7}$$

with k_{i} being the wavenumber of the incident medium.

Equations (6), as representations for the *partial* fields, are valid solutions of Maxwell's equations, excluding the boundary conditions, everywhere in medium p. For the *total* fields, however, similar expressions cannot be written without a careful consideration of the spatial domains in medium p because the boundary conditions have to be imposed. In figure 2, the dashed curves $\tilde{a}_p(x)$ and $\tilde{a}_{p-1}(x)$ are obtained by shifting $a_p(x)$ and $a_{p-1}(x)$ down and up so that they are tangent to $a_{p-1}(x)$ and $a_p(x)$, respectively. In medium p we define three spatial domains as follows:

Ω_p: the space bounded by $a_p(x)$and $a_{p-1}(x)$

Ω_p^+: the space bounded by $a_p(x)$and $\tilde{a}_p(x)$

Ω_p^-: the space bounded by $a_{p-1}(x)$and $\tilde{a}_{p-1}(x)$.

Thus, for the total fields, we have

$$\begin{aligned} \boldsymbol{F}^{(p,p)}(x, u_p) &= \boldsymbol{F}_{+}^{(p,p)}(x, u_p) + \boldsymbol{F}_{-}^{(p,p)}(x, u_p) \\ \boldsymbol{G}^{(p,p)}(x, u_p) &= \boldsymbol{G}_{+}^{(p,p)}(x, u_p) + \boldsymbol{G}_{-}^{(p,p)}(x, u_p) \end{aligned} \qquad (x, u_p) \in \Omega_p^+ \tag{8}$$

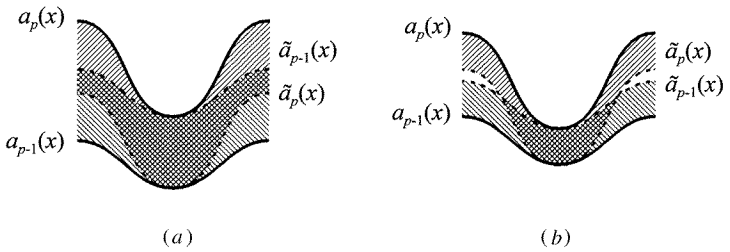

Figure 2. Domains where the full-spectrum expansions for fields are valid. (*a*) The overlap domain covers a full grating period. (*b*) The overlap domain does not cover a full grating period.

and

$$\begin{aligned} \boldsymbol{F}^{(p,p-1)}(x,u_{p-1}) &= \boldsymbol{F}_{+}^{(p,p-1)}(x,u_{p-1}) + \boldsymbol{F}_{-}^{(p,p-1)}(x,u_{p-1}) \\ \boldsymbol{G}^{(p,p-1)}(x,u_{p-1}) &= \boldsymbol{G}_{+}^{(p,p-1)}(x,u_{p-1}) + \boldsymbol{G}_{-}^{(p,p-1)}(x,u_{p-1}) \end{aligned} \qquad (x,u_{p-1}) \in \Omega_p^- . \tag{9}$$

Clearly, in the overlap domain, $\Omega_p^+ \cap \Omega_p^-$ (the cross-hatched domain in figures 2(*a*) and 2(*b*)), both equations (8) and (9) are valid. Outside the domains specified in (8) and (9), these equations may be invalid because the permittivity is not a constant with respect to x. To see that this is true, one only needs to consider the special case in which $a_{p-1}(x)$ represents a horizontal straight line. Then equation (9), when used in domain Ω_p^+, becomes a mathematical statement of the Rayleigh hypothesis. It is worth noting that when the two curves are sufficiently close and their amplitudes are sufficiently different the overlap domain becomes discontinuous with respect to x in either coordinate system (cf figure 2(*b*)).

The virtue of the C method is that it allows the boundary conditions be written simply and accurately by taking advantage of the fact that the medium interface coincides with a coordinate surface of the natural coordinate system. The boundary conditions at $u_p = 0$ are satisfied by requiring

$$\begin{aligned} \boldsymbol{F}^{(p,p)}(x,0) &= \boldsymbol{F}^{(p+1,p)}(x,0) \\ \boldsymbol{G}^{(p,p)}(x,0) &= \boldsymbol{G}^{(p+1,p)}(x,0) . \end{aligned} \tag{10}$$

Or, in terms of scattering matrix,

$$\begin{pmatrix} \nu^{(p+1,p)+} \\ \nu^{(p,p)-} \end{pmatrix} = s'^{(p)} \begin{pmatrix} \nu^{(p,p)+} \\ \nu^{(p+1,p)-} \end{pmatrix} \tag{11}$$

with

$$s'^{(p)} = \begin{pmatrix} F_{mn}^{(p+1,p)+} & -F_{mn}^{(p,p)-} \\ G_{mn}^{(p+1,p)+} & -G_{mn}^{(p,p)-} \end{pmatrix}^{-1} \begin{pmatrix} F_{mn}^{(p,p)+} & -F_{mn}^{(p+1,p)-} \\ G_{mn}^{(p,p)+} & -G_{mn}^{(p+1,p)-} \end{pmatrix} \tag{12}$$

where the superscript (p) of the s' matrix refers to the interface where the boundary conditions are matched.

Equation (11) does not possess a recursive form with respect to the interface number. Referring to figure 3, where the two solid lines schematically represent the two curved interfaces in figure 1, what we have accomplished is crossing the solid line p. If the two interfaces were identical, $\nu_n^{(p,p-1)\pm}$ and $\nu_n^{(p,p)\pm}$ would have been linked one-to-one by an exponential propagating factor, and equation (11) could be easily modified to have the desired recursive form. When the two interfaces are not identical, connecting $\nu_n^{(p,p-1)\pm}$ and

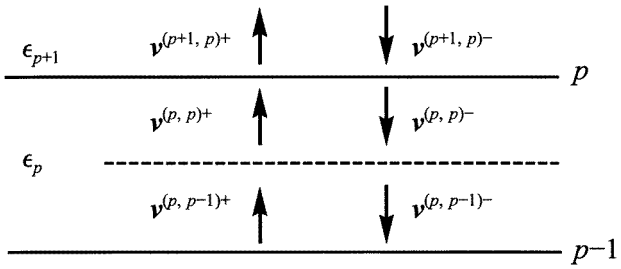

Figure 3. Schematic description of up-waves and down-waves in a layer. The solid lines represent real medium interfaces, and the dashed line represents the need for coordinate transformation.

$v_n^{(p,p)\pm}$ across the dashed line in figure 3 is not so simple, and how to cross the dashed line is the central issue of this paper.

Actually, the problem of layered gratings with two different profiles has been dealt with in the literature for the special case in which one of the interfaces is planar. Two approaches have been taken to represent the fields in the region bounded by a curved interface on one side and a planar interface on the other. Popov and Mashev [5] used the full spectrum of eigensolutions in the curved coordinate system. Li [6] used a sum of the eigensolutions in the Cartesian coordinate system (Rayleigh waves) and the eigensolutions in the curved coordinate system (quasi-Rayleigh waves).

3. Half-spectrum connection methods

The dashed line in figure 3 does not represent a physical boundary. Thus, there are no boundary conditions to be matched. We only need to connect the amplitudes of the field expressed in one coordinate system to the amplitudes of the same field expressed in the other coordinate system, a procedure which we will refer to as field connection.

3.1. The method of Granet et al [4]

In [4], the field connection is accomplished by making the following assumption:

Assumption A. For any (x, u_p) and (x, u_{p-1}) describing the same point in Ω_p,

$$\boldsymbol{F}_{\pm}^{(p,p)}(x, u_p) = \boldsymbol{F}_{\pm}^{(p,p-1)}(x, u_{p-1})\,. \tag{13}$$

(We will discuss the validity of the above assumption later.) The condition for (x, u_p) and (x, u_{p-1}) to describe the same point is

$$u_p + a_p(x) = u_{p-1} + a_{p-1}(x)\,. \tag{14}$$

If we demand that equation (13) be true along a curve u_p = constant, we have

$$\begin{aligned}\boldsymbol{F}_{\pm}^{(p,p)}(x, u_p) &= \boldsymbol{F}_{\pm}^{(p,p-1)}(x, u_p + a_p(x) - a_{p-1}(x)) \\ &= \tilde{\boldsymbol{F}}_{\pm}^{(p,p-1)}(x, u_p)\end{aligned} \tag{15}$$

where

$$\tilde{\boldsymbol{F}}_{\pm}^{(p,q)}(x, u) = \sum_{m,n} \mathrm{e}^{\mathrm{i}\alpha_m x}\, \tilde{F}_{mn}^{(p,q)\pm}\, \mathrm{e}^{\mathrm{i}\lambda_n^{(p,q)\pm} u}\, v_n^{(p,q)\pm} \tag{16}$$

with

$$\tilde{F}_{mn}^{(p,q)\pm} = \sum_l L_{m-l,n}^{(p,q)\pm} F_{ln}^{(p,q)\pm} \tag{17}$$

and

$$L_{mn}^{(p,q)\pm} = \frac{1}{d}\int_0^d \mathrm{e}^{\mathrm{i}\lambda_n^{(p,q)\pm}[a_r(x)-a_q(x)]}\,\mathrm{e}^{-\mathrm{i}mKx}\,\mathrm{d}x\,. \tag{18}$$

In equation (18),

$$r = r(p,q) = \begin{cases} p & \text{if} \quad q = p-1 \\ p-1 & \text{if} \quad q = p\,. \end{cases} \tag{19}$$

Similarly equation (13) taking on u_{p-1} = constant gives,

$$\boldsymbol{F}_{\pm}^{(p,p-1)}(x, u_{p-1}) = \tilde{\boldsymbol{F}}_{\pm}^{(p,p)}(x, u_{p-1})\,. \tag{20}$$

Throughout this paper, we use a tilde above $\boldsymbol{F}^{(p,q)}$ and $\boldsymbol{G}^{(p,q)}$ to denote the vector components of the field that are in coordinate system $r(p,q)$, have (x, u_r) as spatial variables, and are expressed in terms of the eigensolutions in coordinate system q. (G tilde will be needed later in section 4.) It is extremely important that the reader fully understand the above definition of $\tilde{\boldsymbol{F}}^{(p,q)}$ and $\tilde{\boldsymbol{G}}^{(p,q)}$ because they play a crucial role in the definitions of the different field connection methods that we will introduce below.

With the above preparation, the field connection method adopted in [4] can be expressed as (method 1)

$$\boldsymbol{F}_{+}^{(p,p)}(x,0) = \tilde{\boldsymbol{F}}_{+}^{(p,p-1)}(x,0) \tag{21a}$$

$$\tilde{\boldsymbol{F}}_{-}^{(p,p)}(x,0) = \boldsymbol{F}_{-}^{(p,p-1)}(x,0)\,. \tag{21b}$$

In terms of scattering matrix, we have

$$\begin{pmatrix} v^{(p,p)+} \\ v^{(p,p-1)-} \end{pmatrix} = s''^{(p)} \begin{pmatrix} v^{(p,p-1)+} \\ v^{(p,p)-} \end{pmatrix} \tag{22}$$

with

$$s''^{(p)} = \begin{pmatrix} [F_{mn}^{(p,p)+}]^{-1}\tilde{F}_{mn}^{(p,p-1)+} & 0 \\ 0 & [F_{mn}^{(p,p-1)-}]^{-1}\tilde{F}_{mn}^{(p,p)-} \end{pmatrix} \tag{23}$$

where the superscript (p) of the s'' matrix refers to the medium in which the field connection is made. Equation (21) describes a half-spectrum connection method, since the two halves of the eigenvalue spectrum are connected separately. For later reference, we will call it method 1.

By combining $s'^{(p)}$ and $s''^{(p)}$ in the usual way for scattering matrices, a layer scattering matrix can be formed

$$\begin{pmatrix} v^{(p+1,p)+} \\ v^{(p,p-1)-} \end{pmatrix} = s^{(p)} \begin{pmatrix} v^{(p,p-1)+} \\ v^{(p+1,p)-} \end{pmatrix} \tag{24}$$

which has the required recursive form. The whole grating problem can then be solved using the usual recursion formulae for the global scattering matrices.

3.2. Physical consideration about assumption A

From an intuitive physical point of view, assumption A seems very reasonable. Indeed, within layer p there is no physical boundary; therefore, there is no physical mechanism that can turn an up-wave to a down-wave or vice versa. From a fundamental physical point of view, an up-wave or a down-wave is a physical entity (not in a practical sense); therefore, its eigensolution character should be invariant under a coordinate transformation. Note that the coordinate transformation from y to u_p in equation (1) is linear and has a positive unity magnification. Thus, the physical consideration not only supports assumption A, it further suggests a one-to-one correspondence between the waves of the same type in two different coordinate systems.

Unfortunately, the invariance of some of the eigensolutions is severely destroyed by the matrix truncation that is unavoidable in the numerical implementation (for numerical examples, see section 6). Thus, once the matrix truncation is imposed, the eigensolutions are not only physical but also mathematical objects, and assumption A becomes suspect.

3.3. Mathematical consideration about assumption A

Even if the validity of assumption A can be established on physical grounds, equation (13) is not an identity when matrix truncation is imposed. Take equation (20) as an example. The left-hand side contains eigenvalues in $\sigma^{(p,p-1)\pm}$, but the right-hand side contains eigenvalues in $\sigma^{(p,p)\pm}$. We know that for any truncation $\sigma^{(p,p-1)\pm} \neq \sigma^{(p,p)\pm}$. Therefore, equation (20) cannot be satisfied for a continuous variable u_{p-1}. It can only be viewed as an approximate equation.

More importantly, without a proper restriction of the domain of validity, assumption A could lead to the Rayleigh hypothesis. For example, if we apply equation (13) to both the up-waves and the down-waves at the same location $u_p = 0$ we get, (method 2)

$$\boldsymbol{F}_{+}^{(p,p)}(x,0) = \tilde{\boldsymbol{F}}_{+}^{(p,p-1)}(x,0) \tag{25a}$$

$$\boldsymbol{F}_{-}^{(p,p)}(x,0) = \tilde{\boldsymbol{F}}_{-}^{(p,p-1)}(x,0)\,. \tag{25b}$$

In the special case when $a_{p-1}(x)$ represents a horizontal straight line, setting $u_p = 0$ in the first equation of equation (8) and making the substitution of equation (25), we get a mathematical statement of the Rayleigh hypothesis. Note that the Rayleigh hypothesis is cleverly avoided in method 1 by connecting the up-waves and the down-waves at *different* locations.

Next, we consider the asymptotic behaviour of the eigenvalues and eigenvectors. Suppose the Fourier series of the fields are truncated to have P terms symmetrically on both sides of the 0 order. Then, the dimension of matrix $\boldsymbol{M}^{(p,q)}$ is $N = 4P+2$. The numerically computed eigenvalues and eigenvectors therefore depend on N. In this subsection, we use an additional superscript, N, to indicate this dependence. Numerical experiments show that for a fixed constant n,

$$\lim_{N\to\infty} \lambda_n^{(p,q,N)\pm} = \pm\beta_n^{(p)} \tag{26}$$

where $\beta_n^{(p)}$ is the usual y component of the wavenumber in the Rayleigh expansion (the Rayleigh eigenvalue). In equation (26), we have assumed that $\pm\beta_n^{(p)}$ and $\lambda_n^{(p,q,N)\pm}$ have been properly ordered with respect to n. The interesting feature of equation (26) is that the limit is independent of coordinate system q. This is not surprising because in a homogeneous space the eigensolution of Maxwell's equation is just a plane wave and, as remarked in subsection 3.2, the eigenvalue should remain invariant under the coordinate

transformation given by equation (1). It is extremely important to note that the convergence in equation (26) is non-uniform: for equation (26) to be true, n must be a constant. (In the special case of $a_q(x)$ representing a planar surface, the limit sign can be removed.) An expression describing the asymptotic behaviour of the eigenvectors, similar to but much more complicated than equation (26) also exists, but it will be not presented here.

Numerically speaking, for a sufficiently large N approximately half of the eigenvalues in $\sigma^{(p,q,N)}$ that have smaller absolute values (lower order numbers) are equal to the Rayleigh eigenvalues; the other half are very different from the Rayleigh eigenvalues. In fact, the higher-order half generally assumes complex values even for a lossless medium. As has been commented by the previous authors [1, 2], one cannot simply throw away the higher-order half of the eigensolutions. The asymptotic behaviour exhibited in equation (26) is essential to the success of the C method.

The conclusion of this asymptotic analysis is as follows. From a mathematical point of view, althought the convergence of the lower-order half of the spectrum supports assumption A, the non-convergence of the higher-order half of the spectrum destroys its validity. Furthermore, because the higher-order half of the eigensolutions do not have clear physical meaning, it is difficult to use the physical consideration given in subsection 3.2 to support assumption A.

4. Full-spectrum connection method

In subsections 3.2 and 3.3, we have shown that assumption A is essentially based on physical intuition or on the invariance of the eigenvalues of Maxwell's equations, and because of the inevitable matrix truncation occurring in numerical analysis, this assumption is questionable. On the other hand, the laws of physics also require that the total electromagnetic field be covariant under a coordinate transformation. If at a given location the eigenfunction expansions of the total field in two coordinate systems both converge, they should correspond to the same physical field. In other words, they should be related by the tensor transformation rule. Although the covariance of the total field is not exactly preserved due to matrix truncation, its accuracy should improve as the matrix size increases.

Suppose that the two interfaces are sufficiently apart, as in figure 2(*a*). Let $\Delta_p = a_p(x) - \tilde{a}_p(x)$. If we connect the field expressed in coordinate system p and $p-1$ along $\tilde{a}_p(x)$, then we have the full-spectrum connection method, (method 3):

$$\boldsymbol{F}^{(p,p)}(x,-\Delta_p) = \tilde{\boldsymbol{F}}^{(p,p-1)}(x,-\Delta_p) \tag{27a}$$

$$\boldsymbol{G}^{(p,p)}(x,-\Delta_p) = \tilde{\boldsymbol{G}}^{(p,p-1)}(x,-\Delta_p) \tag{27b}$$

where

$$\tilde{\boldsymbol{F}}^{(p,q)}(x,u) = \tilde{\boldsymbol{F}}_+^{(p,q)}(x,u) + \tilde{\boldsymbol{F}}_-^{(p,q)}(x,u) \tag{28a}$$

$$\tilde{\boldsymbol{G}}^{(p,q)}(x,u) = \tilde{\boldsymbol{G}}_+^{(p,q)}(x,u) + \tilde{\boldsymbol{G}}_-^{(p,q)}(x,u) \tag{28b}$$

and

$$\tilde{\boldsymbol{G}}_\pm^{(p,q)}(x,u) = \sum_{m,n} \mathrm{e}^{\mathrm{i}\alpha_m x} \tilde{G}_{mn}^{(p,q)\pm} \mathrm{e}^{\mathrm{i}\lambda_n^{(p,q)\pm} u} \nu_n^{(p,q)\pm} \tag{29}$$

$$\tilde{G}_{mn}^{(p,q)\pm} = \sum_l \left\{ [1 + \dot{a}_r^2]_{m-l} \lambda_n^{(p,q)\pm} - [\dot{a}_r]_{m-l} \alpha_l \right\} \tilde{F}_{ln}^{(p,q)\pm} \tag{30}$$

The integer r in equation (30) is defined in equation (19). Note that the expression of the G tilde matrix above has already taken account of the covariant change of the vector

component. Equation (27*b*) is necessary because equation (27*a*) alone is insufficient for uniquely determining a scattering matrix relating $v_n^{(p,p-1)\pm}$ and $v_n^{(p,p)\pm}$. Now, to replace equation (23) we have

$$s''^{(p)} = \begin{pmatrix} \mathrm{e}^{\mathrm{i}\lambda_m^{(p,p)+}\Delta_p} & 0 \\ 0 & 1 \end{pmatrix} \begin{pmatrix} F_{mn}^{(p,p)+} & -\hat{F}_{mn}^{(p,p-1)-} \\ G_{mn}^{(p,p)+} & -\hat{G}_{mn}^{(p,p-1)-} \end{pmatrix}^{-1} \times \begin{pmatrix} \hat{F}_{mn}^{(p,p-1)+} & -F_{mn}^{(p,p)-} \\ \hat{G}_{mn}^{(p,p-1)+} & -G_{mn}^{(p,p)-} \end{pmatrix} \begin{pmatrix} 1 & 0 \\ 0 & \mathrm{e}^{-\mathrm{i}\lambda_n^{(p,p)-}\Delta_p} \end{pmatrix} \tag{31}$$

where

$$\hat{F}_{mn}^{(p,p-1)\pm} = \tilde{F}_{mn}^{(p,p-1)\pm} \mathrm{e}^{-\mathrm{i}\lambda_n^{(p,p-1)\pm}\Delta_p} \tag{32a}$$

$$\hat{G}_{mn}^{(p,p-1)\pm} = \tilde{G}_{mn}^{(p,p-1)\pm} \mathrm{e}^{-\mathrm{i}\lambda_n^{(p,p-1)\pm}\Delta_p} . \tag{32b}$$

If the situation as shown in figure 2(*b*) occurs, the full-spectrum connection method *a priori* cannot be applied. This is because in this case equations (27) are only valid over a portion of the grating period, the completeness of the Fourier basis cannot be used to derive the matrix equation (31) from the functional equations (27).

5. Hybrid-spectrum connection method

Assumption A given in section 4 can be replaced by a new assumption below:

Assumption B. At any point (x, y) in Ω_p, the total field, $\boldsymbol{F}^{(p)}$, is given by

$$\boldsymbol{F}^{(p)}(x, y) = \boldsymbol{F}_+^{(p,p-1)}(x, u_{p-1}(y)) + \boldsymbol{F}_-^{(p,p)}(x, u_p(y)) . \tag{33}$$

This assumption was conceived by extracting the useful information from method 1 as specified by equations (21) and by extending the successful procedure reported in the literature in treating the transition between a curvilinear coordinate system and the Cartesian coordinate system [1, 2, 6]. Similar to the case of assumption A, it is difficult to mathematically prove the validity of assumption B. Nonetheless, its physical meaning is clear: the total field everywhere in a layer is given by the superposition of all scattered waves from the two boundaries. In medium p, the sum of scattered waves from interface $p-1$ is $\boldsymbol{F}_+^{(p,p-1)}$, and that from interface p is $\boldsymbol{F}_-^{(p,p)}$.

There are several advantages in using assumption B over assumption A. (i) Assumption B avoids the danger of invoking the Rayleigh hypothesis. (ii) Assumption A can be derived from assumption B with the proper restriction of the domains of validity imposed. (iii) Equation (33) can be used directly to match boundary conditions, eliminating the need to connect fields, as demonstrated below.

Using field representation equation (33) to satisfy the continuity of E_z across interface p, we have (method 4)

$$\boldsymbol{F}_+^{(p+1,p)}(x, 0) + \tilde{\boldsymbol{F}}_-^{(p+1,p+1)}(x, 0) = \tilde{\boldsymbol{F}}_+^{(p,p-1)}(x, 0) + \boldsymbol{F}_-^{(p,p)}(x, 0) . \tag{34a}$$

It is easy to see that the corresponding continuity equation for H_x is

$$\boldsymbol{G}_+^{(p+1,p)}(x, 0) + \tilde{\boldsymbol{G}}_-^{(p+1,p+1)}(x, 0) = \tilde{\boldsymbol{G}}_+^{(p,p-1)}(x, 0) + \boldsymbol{G}_-^{(p,p)}(x, 0) . \tag{34b}$$

From the two equations above, the scattering matrix $s^{(p)}$ in equation (24) can be derived:

$$s^{(p)} = \begin{pmatrix} F_{mn}^{(p+1,p)+} & -F_{mn}^{(p,p)-} \\ G_{mn}^{(p+1,p)+} & -G_{mn}^{(p,p)-} \end{pmatrix}^{-1} \begin{pmatrix} \tilde{F}_{mn}^{(p,p-1)+} & -\tilde{F}_{mn}^{(p+1,p+1)-} \\ \tilde{G}_{mn}^{(p,p-1)+} & -\tilde{G}_{mn}^{(p+1,p+1)-} \end{pmatrix} . \tag{35}$$

In comparison with the other methods, where the layer scattering matrix $s^{(p)}$ is constructed in two steps, here only one step is needed. It is also worth noting that half of the eigenvectors of $M^{(p,q)}$, i.e. $\left(F_{mn}^{(p,p)+}, G_{mn}^{(p,p)+}\right)$ and $\left(F_{mn}^{(p,p-1)-}, G_{mn}^{(p,p-1)-}\right)$ are never used in method 4.

6. Numerical examples

In this section, we first present a brief numerical investigation concerning the validity of assumption A. Then, we give some results of the convergence of diffraction efficiencies computed by the four field connection methods defined previously. For simplicity, we only consider single-layered gratings, which can be obtained by setting $p = 2$ in figure 1. The two medium interfaces, except for cases in tables 7 and 8, are described by

$$a_1(x) = \frac{h_1}{2}\cos Kx \qquad a_2(x) = \frac{h_2}{2}\cos Kx + e_2\,. \tag{36}$$

If we consider that the full-spectrum connection method is more reliable than the half-spectrum connection method on physical and mathematical grounds, then we can numerically investigate the validity of assumption A. From equation (27), we have

$$\begin{pmatrix} \nu_m^{(p,p)+}\mathrm{e}^{-\mathrm{i}\lambda_m^{(p,p)+}\Delta_p} \\ \nu_m^{(p,p)-}\mathrm{e}^{-\mathrm{i}\lambda_m^{(p,p)-}\Delta_p} \end{pmatrix} = \begin{pmatrix} t_{11}^{(p)} & t_{12}^{(p)} \\ t_{21}^{(p)} & t_{22}^{(p)} \end{pmatrix}\begin{pmatrix} \nu_n^{(p,p-1)+} \\ \nu_n^{(p,p-1)-} \end{pmatrix} \tag{37}$$

with

$$\begin{pmatrix} t_{11}^{(p)} & t_{12}^{(p)} \\ t_{21}^{(p)} & t_{22}^{(p)} \end{pmatrix} = \begin{pmatrix} F_{mn}^{(p,p)+} & F_{mn}^{(p,p)-} \\ G_{mn}^{(p,p)+} & G_{mn}^{(p,p)-} \end{pmatrix}^{-1}\begin{pmatrix} \hat{F}_{mn}^{(p,p-1)+} & \hat{F}_{mn}^{(p,p-1)-} \\ \hat{G}_{mn}^{(p,p-1)+} & \hat{G}_{mn}^{(p,p-1)-} \end{pmatrix}. \tag{38}$$

Thus, the two off-diagonal sub-matrices, $t_{21}^{(p)}$ and $t_{12}^{(p)}$, couple the up-waves and the down-waves of coordinate system $p-1$ along curve $u_{p-1} = 0$ to the down-waves and up-waves of coordinate system p along curve $u_p = -\Delta_p$ respectively. According to assumption A, these off-diagonal blocks should be zero.

In figure 4, the sub-matrices t_{11}^2 and $t_{12}^{(2)}$ are 'plotted'. The horizontal and vertical axes represent the row and column positions. If the absolute value of a matrix element is greater than 10^{-6} (double precision is used here), its position is marked by a dot; otherwise the position is unmarked. It is evident that as the matrix dimension increases, the lower-order half of the up-waves are only coupled to the up-waves of the same order; however, the higher-order half of the up-waves not only couple to the up-waves of other higher orders they also couple to the down-waves of high orders.

Next, we consider the convergence of diffraction efficiencies computed by the four field connection methods for the following four different grating cases.

Case 1. Sinusoidal gratings, grating period $d = 1.5$, groove depths h_1, $h_2 = 0.2$, 2.0, wavelength $\lambda = 1.0$, incident angle $\theta = 15^\circ$, permittivities $\epsilon_1 = \epsilon_3 = 1.0$, $\epsilon_2 = 2.25$.

Case 2. Sinusoidal gratings, grating period $d = 1.3$, groove depths h_1, $h_2 = 0.1$, 1.0, wavelength $\lambda = 0.55$, incident angle $\theta = 30^\circ$, permittivities $\epsilon_1 = 2.25$, $\epsilon_2 = 4.0$, $\epsilon_3 = 1.0$.

Case 3. Sinusoidal gratings, grating period $d = 1.3$, groove depths h_1, $h_2 = 0.1$, 1.0, wavelength $\lambda = 0.55$, incident angle at the second order Littrow, permittivities $\epsilon_1 = -25$, $\epsilon_2 = 2.25$, $\epsilon_3 = 1.0$.

Case 4. Triangular gratings, grating period $d = 2.0$, $d_1 = 0.5$ (d_1 is the horizontal distance between a minimum of the profile and the nearest maximum on its right side), groove

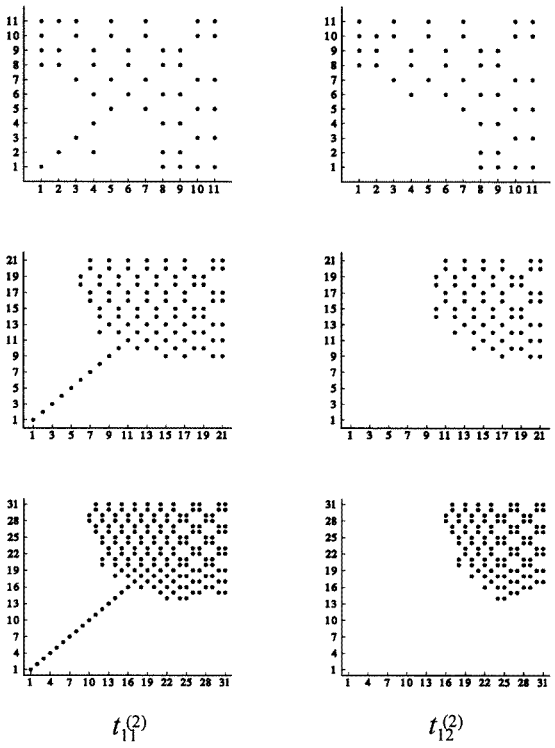

Figure 4. Schematic representation of the sparseness of the sub-matrices $t_{11}^{(2)}$ and $t_{12}^{(2)}$ for a grating that is defined in case 1, except that $h_1 = 0.2$ and $h_2 = 0.1$. Here, e_2 is irrelevant and the polarization is TE.

depths h_1, $h_2 = 0.1$, 0.5, wavelength $\lambda = 1.0$, incident angle $\theta = 45^\circ$ permittivities $\epsilon_1 = 2.25$, $\epsilon_2 = 4.0$, $\epsilon_3 = 1.0$.

Case 1 is basically taken from [4]. It is a relatively easy case because there are only three diffraction orders in both semi-infinite media, although we have chosen the larger groove depth to be greater than the grating period in order to make the convergence of the computer codes more demanding. Case 2 is more stringent than case 1 because it allows many more propagating orders. The substrate in case 3 is metallic, but we intentionally set the imaginary part of ϵ_1 to zero so that the grating is lossless. For case 4, we have considerably reduced the grating groove depths because the convergence rate of the C method is much slower for a triangular profile than for the sinusoidal profile, for the same groove depth.

Tables 1–4 give the absolute values of the differences between unity and the sums of all diffraction efficiencies that are computed by our computer programs based on the four field connection methods. In these tables the spacing e_2 between the two interfaces is specified by a parameter γ:

$$e_2 = (\gamma + 0.5)|h_1 - h_2| \,. \tag{39}$$

Thus, when $\gamma = 0$ the two interfaces are tangent to each other, and $\gamma = 1$ gives the minimum e_2 such that the overlap domain in figure 2(*a*) spans a full grating period. The integers in parentheses are base 10 exponents. For these results, $P = 20$.

Table 1. Errors in conservation of energy (TE polarization) by different field connection methods for the sinusoidal gratings in case 1.

Field connection method ($h_1 = 0.2$, $h_2 = 2.0$)	$\gamma = 0.0$	$\gamma = 0.5$	$\gamma = 1.0$	$\gamma = 1.5$
1	6.9(−6)	2.6(−8)	4.5(−8)	1.3(−8)
2	$\gg 0$	$\gg 0$	$\gg 0$	$\gg 0$
3	$\gg 0$	$\gg 0$	3.6(−3)	2.8(−3)
4	1.3(−5)	9.6(−9)	4.4(−8)	1.1(−8)
Field connection method ($h_1 = 2.0$, $h_2 = 0.2$)	$\gamma = 0.0$	$\gamma = 0.5$	$\gamma = 1.0$	$\gamma = 1.5$
1	1.1(−4)	1.2(−6)	2.0(−7)	9.5(−7)
2	3.9(−5)	3.1(−5)	3.7(−5)	2.6(−5)
3	3.3(−4)	4.8(−4)	1.5(−4)	4.0(−5)
4	1.0(−4)	1.2(−6)	2.1(−7)	9.4(−7)

Table 2. Errors in conservation of energy (TE polarization) by different field connection methods for the sinusoidal gratings in case 2.

Field connection method ($h_1 = 0.1$, $h_2 = 1.0$)	$\gamma = 0.0$	$\gamma = 0.5$	$\gamma = 1.0$	$\gamma = 1.5$
1	3.7(−6)	1.1(−6)	2.0(−6)	1.0(−6)
2	$\gg 0$	$\gg 0$	$\gg 0$	$\gg 0$
3	$\gg 0$	$\gg 0$	$\gg 0$	$\gg 0$
4	6.0(−6)	1.1(−6)	2.2(−6)	1.0(−6)
Field connection method ($h_1 = 1.0$, $h_2 = 0.1$)	$\gamma = 0.0$	$\gamma = 0.5$	$\gamma = 1.0$	$\gamma = 1.5$
1	5.1(−6)	1.9(−7)	3.2(−7)	2.6(−7)
2	7.7(−5)	2.4(−6)	3.9(−6)	1.8(−4)
3	5.2(−4)	5.2(−6)	1.2(−4)	1.8(−5)
4	2.0(−6)	1.2(−7)	3.2(−7)	1.4(−7)

Our experience has shown that when the C method is extended to treat gratings of non-identical profiles, the error in conservation of energy is a good indicator for the convergence of efficiencies of individual diffraction orders. Furthermore, the convergence behaviour of the C method is virtually independent of polarization. Therefore, the convergence behaviours of the errors in energy conservation that are shown in tables 1–4 are representative for the convergence of diffraction efficiencies in both polarizations.

It can be easily seen from tables 1, 2 and 3 that method 1 and method 4 converge well in all three cases, for all combinations of h_1, h_2 and γ. As predicted, method 2 fails in all three cases and all γ values, so long as $h_1 \ll h_2$. Also as predicted, method 3 fails in all three cases when $h_1 \ll h_2$ and $\gamma < 1.0$. When $h_1 \ll h_2$ and $\gamma \geqslant 1.0$, its also fails in case 2, the most stringent case. Interestingly, all methods converge well when $h_1 \gg h_2$, regardless of the grating case and γ value. Table 4 shows that both methods 1 and 4 coverged for the triangular gratings. The results for methods 2 and 3 are not included because they failed to converge for all combinations of h_1, h_2 and γ. This failure of convergence is believed to be related to the slow convergence of the C method for triangular gratings.

Table 3. Errors in conservation of energy (TE polarization) by different field connection methods for the sinusoidal gratings in case 3.

Field connection method ($h_1 = 0.1$, $h_2 = 1.0$)	$\gamma = 0.0$	$\gamma = 0.5$	$\gamma = 1.0$	$\gamma = 1.5$
1	3.7(−8)	1.2(−7)	2.0(−7)	2.0(−7)
2	$\gg 0$	$\gg 0$	$\gg 0$	$\gg 0$
3	$\gg 0$	$\gg 0$	6.5(−5)	2.9(−4)
4	1.0(−7)	1.0(−7)	2.0(−7)	2.0(−7)
Field connection method ($h_1 = 1.0$, $h_2 = 0.1$)	$\gamma = 0.0$	$\gamma = 0.5$	$\gamma = 1.0$	$\gamma = 1.5$
1	8.6(−4)	8.5(−4)	2.1(−3)	1.0(−3)
2	2.2(−3)	8.5(−4)	2.1(−3)	1.0(−3)
3	6.2(−3)	1.6(−3)	4.5(−3)	1.7(−3)
4	8.6(−4)	8.5(−4)	2.1(−3)	1.0(−3)

Table 4. Errors in conservation of energy (TE polarization) by field connection methods 1 and 4 for the triangular gratings in case 4.

Field connection method ($h_1 = 0.1$, $h_2 = 0.5$)	$\gamma = 0.0$	$\gamma = 0.5$	$\gamma = 1.0$	$\gamma = 1.5$
1	4.4(−4)	6.9(−3)	8.9(−4)	1.1(−2)
4	6.7(−4)	6.3(−3)	5.3(−4)	1.1(−2)
Field connection method ($h_1 = 0.5$, $h_2 = 0.1$)	$\gamma = 0.0$	$\gamma = 0.5$	$\gamma = 1.0$	$\gamma = 1.5$
1	7.6(−4)	5.6(−3)	6.0(−4)	1.4(−2)
4	3.2(−3)	1.8(−2)	5.0(−3)	1.8(−2)

Table 5. Diffraction efficiencies of the sinusoidal gratings in case 1 ($\gamma = 0.0$).

	TE		TM	
Diffraction order	$h_1 = 0.2$ $h_2 = 2.0$	$h_1 = 2.0$ $h_2 = 0.2$	$h_1 = 0.2$ $h_2 = 2.0$	$h_1 = 2.0$ $h_2 = 0.2$
R, −1	0.2591(−1)	0.5726(−2)	0.8168(−2)	0.2805(−1)
R, 0	0.8379(−1)	0.1754(−1)	0.3718(−2)	0.2240(−1)
R, +1	0.1074	0.1885(−1)	0.1072(−2)	0.1812(−1)
T, −1	0.2433	0.5632	0.5478	0.7186
T, 0	0.3110	0.3110	0.1277	0.1276
T, +1	0.2286	0.8376(−1)	0.3116	0.8568(−1)

In tables 5–8, we give both the TE and TM diffraction efficiency values for the two gratings with $\gamma = 0$ in the four cases. Again, $P = 20$ was used in the computation. In figure 5, the convergence of the error in conservation of energy in the first TE case of table 5 is plotted against the matrix truncation parameter P. As has been shown in tables 1–4, methods 1 and 4 have approximately the same convergence rate.

When $h_1 < h_2$, the field connection method 2 can be thought of as giving rise to the generalized Rayleigh–Fourier (RF) method in the sense that it expands the field along a

Table 6. Diffraction efficiencies of the sinusoidal gratings in case 2 ($\gamma = 0.0$).

	TE		TM	
Diffraction order	$h_1 = 0.1$ $h_2 = 1.0$	$h_1 = 1.0$ $h_2 = 0.1$	$h_1 = 0.1$ $h_2 = 1.0$	$h_1 = 1.0$ $h_2 = 0.1$
R, −3	0.2512(−1)	0.4026(−2)	0.5903(−2)	0.7557(−3)
R, −2	0.3680(−2)	0.1638(−2)	0.1348(−1)	0.1944(−2)
R, −1	0.4111(−4)	0.2739(−1)	0.1043(−2)	0.3463(−1)
R, 0	0.2982(−1)	0.9792(−1)	0.7318(−2)	0.3035(−1)
R, +1	0.3766(−1)	0.2516(−1)	0.7741(−2)	0.1123(−1)
T, −4	0.5900(−1)	0.6827(−1)	0.1522(−1)	0.7337(−1)
T, −3	0.6359(−1)	0.4309(−1)	0.1517	0.1472(−1)
T, −2	0.6209(−1)	0.1283	0.2634(−1)	0.1220
T, −1	0.2633(−1)	0.2945	0.1184	0.3988
T, 0	0.2733	0.2306(−1)	0.3911(−1)	0.1208(−2)
T, +1	0.1099	0.1271	0.1387	0.9560(−1)
T, +2	0.3667	0.1595	0.4750	0.2153

Table 7. Diffraction efficiencies of the sinusoidal gratings in case 3 ($\gamma = 0.0$)

	TE		TM	
Diffraction order	$h_1 = 0.1$ $h_2 = 1.0$	$h_1 = 1.0$ $h_2 = 0.1$	$h_1 = 0.1$ $h_2 = 1.0$	$h_1 = 1.0$ $h_2 = 0.1$
R, −3	0.1340	0.1236	0.1099	0.2729
R, −2	0.1432	0.2460	0.3258(−1)	0.4422
R, −1	0.4290(−1)	0.4089(−1)	0.2107(−1)	0.2798(−1)
R, 0	0.5781	0.4566	0.7413	0.1682
R, +1	0.1018	0.1337	0.9517	0.8848(−1)

Table 8. Diffraction efficiencies of the triangular gratings in case 4 ($\gamma = 0.0$)

	TE		TM	
Diffraction order	$h_1 = 0.1$ $h_2 = 0.5$	$h_1 = 0.5$ $h_2 = 0.1$	$h_1 = 0.1$ $h_2 = 0.5$	$h_1 = 0.5$ $h_2 = 0.1$
R, −3	0.134(−1)	0.242(−2)	0.286(−1)	0.114(−2)
R, −2	0.142(−1)	0.253(−2)	0.125(−1)	0.229(−2)
R, −1	0.378(−1)	0.831(−2)	0.100(−1)	0.360(−2)
R, 0	0.254(−1)	0.211	0.381(−2)	0.348(−1)
T, −4	0.338(−2)	0.459(−3)	0.392(−2)	0.276(−2)
T, −3	0.283(−2)	0.868(−3)	0.828(−3)	0.128(−2)
T, −2	0.876(−3)	0.357(−2)	0.199(−2)	0.360(−2)
T, −1	0.291	0.237(−1)	0.247	0.287(−1)
T, 0	0.291	0.698	0.326	0.876
T, +1	0.320	0.477(−1)	0.362	0.496(−1)

grating profile of larger amplitude h_2 in terms of the eigensolutions of Maxwell's equations in a coordinate system generated by a grating profile of smaller amplitude h_1. We then may say that when $h_1 > h_2$ method 2 gives rise to the reverse generalized RF method. It is interesting to observe from tables 1–3 that, as is true for the traditional RF method for

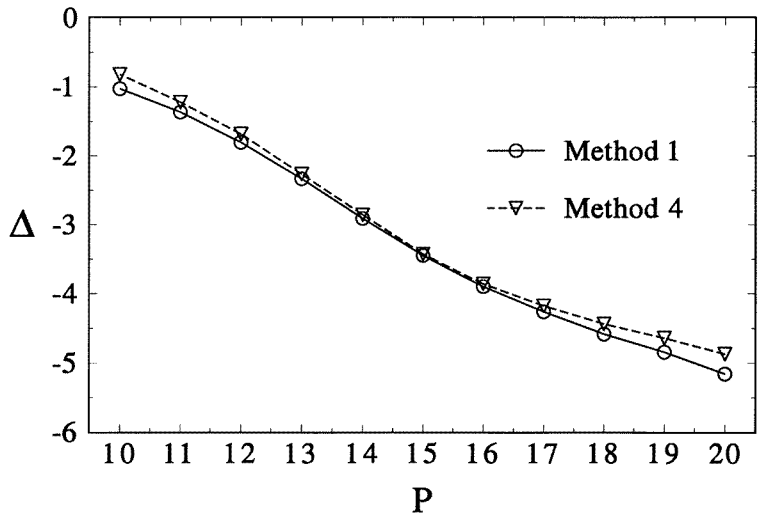

Figure 5. Convergence of the error in conservation of energy for methods 1 and 4. The error is measured by $\Delta = \log_{10}|1 - \sum \eta_i|$, where η_i are diffraction efficiencies.

which $h_1 = 0$, the generalized RF method fails when $h_1 \ll h_2$ for a sufficiently large h_2; however, surprisingly the reverse RF method always works.

The four grating cases that we have studied here are characterized by the large difference between the two groove depths in each pair. We designed these cases this way for the purpose of exploring the limitations of the field connection methods. It is worth mentioning that when the difference between the groove depths is small all four methods work well.

7. Discussion

The physical, mathematical and numerical analysis that we have presented so far may seem to be contradictory: assumption A is physically plausible but mathematically questionable. Furthermore, the preceding section has shown that method 1, which is based on assumption A, numerically works well. The key to resolving this ambiguity is to understand the role that matrix truncation plays in the numerical process. Physics and rigorous mathematics tell us that there is a one-to-one correspondence between the eigensolutions of finite order number in two different coordinate systems. The corollary of the above statement is that (in the appropriate spatial domains) there is an equality between the sums of finite number of up-waves (down-waves) in two different coordinate systems. However, once matrix truncation is imposed, these relationships are partially destroyed.

Thus, there are at least three options: (i) Insist on having the one-to-one correspondence even in the case of finite matrix and use the limiting eigensolutions in the numerical solution. (ii) Abandon the one-to-one correspondence but keep the equality of the partial sums. (iii) Abandon both the equality of the partial sums and the one-to-one correspondence, and rely on the covariance of the total field. It is well known that the first option is the Rayleigh hypothesis. In the third option, both $\boldsymbol{F}^{(p)}$ and $\boldsymbol{G}^{(p)}$ in two coordinate systems have to be connected. With matrix truncation, this field connection method effectively creates a discontinuous numerical interface and introduces numerical coupling between the up-waves and the down-waves. Thus, although it appears to rest on a solid physical and mathematical

ground, it is numerically ineffective. The second option, when implemented correctly to avoid the Rayleigh hypothesis, seems to strike just the right balance.

8. Conclusions

We have carefully examined the validity of assumption A. From a physical point of view the assumption is reasonable, but from a mathematical point of view it is, in general, invalid. Without the proper restriction of the spatial domains to which the assumption is applied, it may lead to the Rayleigh hypothesis.

We have numerically investigated the performance of four field connection methods to extend the C method to coated gratings of different profiles. We find that both the half-spectrum method proposed in [4] and the hybrid-spectrum method newly proposed in this paper have excellent convergence property for all grating configurations that we have subjected them to, some of which are quite stringent, but the other two methods have much smaller range of applicability.

This research has raised some interesting questions. For example, why does the reverse Rayleigh–Fourier method work well for deep gratings, while the Rayleigh–Fourier method does not? We have conducted this research relying mostly on numerical analysis. An analytical study is desirable, but it may be difficult. Also, we have only analysed the convergence of diffraction efficiencies. A convergence study of the near fields may provide some insights to the complex and subtle issues addressed in this paper.

References

[1] Chandezon J, Maystre D and Raoult G 1980 *J. Optique* **11** 235–41
[2] Chandezon J, Dupuis M T, Cornet G and Maystre D 1982 *J. Opt. Soc. Am.* **72** 839–46
[3] Avrutsky I A, Svakhin A S and Sychugov V A 1989 *J. Mod. Opt.* **36** 1303–20
[4] Granet G, Plumey J P and Chandezon J 1995 *Pure Appl. Optics* **4** 1–5
[5] Popov E and Mashev L 1986 *J. Opt. Commun.* **7** 127–31
[6] Li L 1994 *J. Opt. Soc. Am.* **11** 2816–28